European Journal of Wood and Wood Products (2025) 83:156
https://doi.org/10.1007/s00107-025-02309-w

ORIGINAL ARTICLE

Investigating impact behavior of silver birch and black locust clear wood using digital image correlation

Mojtaba Hassan Vand[1] · **Jan Tippner**[1]

Received: 13 November 2024 / Accepted: 23 July 2025

Abstract

This study investigates the mechanical properties and the deformation pattern of silver birch (*Betula pendula*) and black locust (*Robinia pseudoacacia*) wood species under impact loading conditions. A drop-release impact testing machine tested the specimens in 3-point bending while a high-speed camera recorded the impact events. Subsequently, the recorded images were processed using the digital image correlation method to analyze deformation and strain behaviour. Basic physical properties of the specimens were determined, alongside test results such as maximum dynamic applied force, maximum deflection, and maximum normal tensile strain up to breakage. Also, the impact bending strength of the specimens was assessed. The maximum deflection and normal tensional strain of them were comparable. Both species had a similar impact bending strength value. Additionally, both species' normal and shear strain distributions were determined for three levels of deflection in bending. This research contributes to a deeper understanding of these two wood species' response to dynamic loadings, facilitating the development of more accurate predictive models and engineering designs.

1 Introduction

Birch (*Betula pendula*) is considered one of the premier species for land reclamation and revegetation endeavours, owing to its exceptional attributes such as its remarkable tolerance to a wide range of environmental conditions, its ability to flourish even in nutrient-poor soils, and its capacity to provide protection for the seedlings of both broadleaved and coniferous tree species (Beck et al. 2016). Its high resistance to chemical pollutants makes it a valuable candidate for reclaiming degraded areas, serving as an efficient tool for restoring lands affected by industrial activities through afforestation methods (Jonczak et al. 2020). Regarding its wood properties, birch is generally classified as medium-hard timber with good mechanical properties (Borůvka et al. 2019). However, birch is highly vulnerable to wood fungi and has low dimensional stability, limiting its applications only to indoor applications, such as furniture or as a source of fuel for heat generation (Biziks et al. 2013; Borůvka et al. 2018). However, its water repellence can be enhanced to certain levels (Yin et al. 2021). Although birch solid wood is unsuitable as a construction material due to its limitations, birch can be used in different forms to craft various furniture components requiring exceptional stiffness and strength, particularly for indoor applications (Heräjärvi 2004). Birch has a rich history in the veneer industry due to its unique properties (Dudík et al. 2020), which is further advancing thanks to new methods of wood treatment (Grinins et al. 2016). Birch has excellent robustness against impacts, demonstrated by its ability to absorb significant amounts of impact energy (Bragov and Lomunov 1997). Studies indicate that its laminated composites exhibit greater resilience against dynamic compressive crashes compared to composites made of poplar and oak (Guélou et al. 2023). Birch's notable strength against impacts and its capacity to efficiently absorb impact energy across varied environmental conditions make it a promising candidate material for diverse automotive applications (Baumann et al. 2020, 2021).

Black locust (*Robinia pseudoacacia* L.) was the first forest tree species introduced from North America to Europe four centuries ago; now, it has widespread cultivation not only in Europe but also across diverse global climatic regions (Rédei et al. 2008). Despite its extensive planting, this species is considered invasive in central Europe and

✉ Mojtaba Hassan Vand
xhassanv@mendelu.cz

[1] Department of Wood Science and Technology, Faculty of Forestry and Wood Technology, Mendel University in Brno, Zemědělská 3, 613 00 Brno, Czech Republic

Published online: 20 August 2025

is included on national blacklists and inventories of alien species throughout the continent (Younis et al. 2023). Its global ecological importance is due to its ability to enhance soil chemical properties and fertility through nitrogen fixation and carbon sequestration (Nicolescu et al. 2018). Black locust demonstrates resilience to drought and harsh environmental conditions, and the ongoing climatic changes appear to favour its adaptation further and spread (Grünewald et al. 2009). However, the black locust brings about both positive and negative impacts, representing a substantial influence across various domains such as nature conservation, afforestation, urban landscaping, timber and fuel production, and beekeeping (Gilman and Watson 1994).

Black locust wood is characterized as a relatively dense, hard and durable ring-porous hardwood featuring light yellow sapwood and darker greenish-yellow heartwood with black pores (Adamopoulos et al. 2007). Its mechanical properties improve with the tree's age (Bijak and Lachowicz 2021). While its wood holds significant potential as a cost-effective fuel in the form of firewood, its durability and resistance to rot and insect damage make it a suitable material for various applications, including outdoor constructions, boatbuilding, indoor flooring and furniture, mine timbers, railway sleepers, and veneer (Sitzia et al. 2016). Their unique resistance is becoming more valuable due to insufficient production of durable timbers from other parts of the world, such as Africa, and the availability of black locusts with durable timber in Europe (Dünisch et al. 2010). Renowned for its rapid growth, durability, malleability, ductility, and versatility, black locust ranks among Hungary's most esteemed trees (Csordós et al. 2014). The Young's modulus, yield stress, and modulus of rupture of black locust are lower for sapwood compared to heartwood (Niklas 1997), and its elastic and shear moduli remain unaffected by radial and tangential orientation in static state loadings (Adamopoulos 2002). Heat treatment can make black locust more resistant to different hazards; however, this process can damage its mechanical properties. For instance, its average impact bending strength values can diminish by 45–70% by oil heat treatment, depending on the type of treatment applied (Bak and Nemeth 2012).

Wood has a considerable application across various industries, including aircraft, automotive, packaging, construction and sporting goods production, and in some of these sections, it is often subjected to dynamic loadings (impacts) (Polocoer et al. 2017; Jansson 1992). However, utilization of wood in society was notably more significant before the exponential multiplication of synthetic materials (Johnson 1986). Dynamic regime loadings encompass strain rates from 0.1 to 10^4, covering various impact testing methods (Field et al. 2004; Jacques et al. 2014). Wood is a strain rate-dependent material due to its viscoelastic polymer components and structure, exhibiting softening under creep and strengthening under dynamic loading (Matsushita et al. 2020). In various fields of application, the severity of the incidents can be mitigated by using energy-absorbing protective materials like wood (Bragov et al. 2006). Wood is progressively receiving increased attention due to its low cost, lightweight nature, eco-friendliness, renewability, and ability to efficiently absorb high-rate loadings, shocks, impacts, and explosive forces (Bragov et al. 2020). The energy absorbed from low-energy impacts is mainly attributed to the buckling and collapse of cell walls in compression beneath the projectile (Hepworth et al. 2002). Moreover, the energy absorption capacity of wood increases with strain rate, making it suitable for a wide range of loadings (Wouts et al. 2016). Also, wood has potential to be modified and improved against impacts and high-rate loadings (Wight et al. 2024, 2025; Cao et al. 2024). The ability to absorb energy is quantified by the impact bending strength (IBS), where a high value signifies high strength and a fibrous fracture pattern in wooden samples, while a low IBS indicates a blunt fracture in brittle wood samples (Gaff et al. 2016). IBS is regarded as a mechanical property similar to others, like modulus of elasticity; however, it is linked explicitly to dynamic loading, unlike other properties associated with static loadings (Bal 2021).

Traditional methods for measuring the distribution of strain and deflection, such as mechanical and electronic strain gauges have disadvantages such as time consumption, tedium, difficulty, and, in some cases, inaccuracy, often due to equipment limitations (Zink et al. 1995). In contrast, the digital image correlation method (DIC) is more efficient and it obliterates many of these common problems, offering a wide range of abilities (Keunecke et al. 2012). DIC involves capturing images of an object during tests, storing them digitally, and then analysing them using suitable algorithms and equipment to extract full-field shape, deformation, and motion measurements (Sutton et al. 2009). The fundamental principle of DIC is tracking the same points in the input images before and after deformation using techniques like cross-correlation or the sum of squared differences (Moilanen et al. 2015). However, DIC does have limitations such as its sensitivity to testing environment conditions and presenting difficulties in sample preparation (Górszczyk et al. 2019).

DIC offers interesting advantages over traditional strain measurement methods. Firstly, it enables contactless strain measurement, eliminating the need for physical contact with the specimen. Secondly, DIC can capture full-field strain of all points in a single process, providing a clear viewpoint toward strain distribution. Thirdly, DIC is not influenced by the rigid motion of specimens. Fourthly, DIC eliminates the need for strain gauges, which are typically single-use devices in impact tests, thereby decreasing the cost (Dave et al. 2018). Although DIC is already considered a common tool for assessing wooden materials under various static tests, its application in dynamic loadings has been limited by technical limitations related to high-speed image recording (Pierron et al. 2011). However, recent advancements in high-speed camera technology have made it feasible to use DIC for evaluating dynamic loadings and impacts, regardless of strain rate (Wouts et al. 2016). DIC has demonstrated outstanding potential for assessing the impact bending of wood, enabling measurement of deflection, shear, and normal strain distribution everywhere of a specimen (Hassan Vand et al. 2024). Additionally, DIC can be used to study fracture and crack propagation in wood (Thuvander et al. 2000).

This study aimed to provide a clear viewpoint of the mechanical properties of two wood species under dynamic loading conditions. Specifically, we measured their key parameters, such as IBS and the maximum dynamic applied force required for crack initiation from the impact testing machine. Additionally, we measured the deflection and the normal and shear strain distribution of the samples by the DIC method. Through these assessments, we aimed to gain comprehensive information about the performance and suitability of these wood species for applications that may be subject to dynamic loads, thereby assessing their potential for being used in various applications. Nevertheless, this study omitted the quantification of strain-rate effects by not comparing the impact tests with corresponding quasi-static data.

2 Materials and methods

2.1 Preparation of the samples

Boards of silver birch and black locust were provided for this study from enterprises in the South Moravia region of the Czech Republic. Small, clear samples, without any knots and defects, were cut from these boards into beams with 20 × 20 × 300 mm dimensions. The specimens were conditioned to have 11% of moisture content (MC) by storing them in an environmental chamber maintained at 20 °C and 65% relative humidity. The specimens were painted with a grayscale random speckled pattern to enhance the efficiency of the DIC method, since the accuracy of DIC is closely related to the quality of the speckled pattern (Pan et al. 2009).

2.2 Impact tests configuration

The impact tests were conducted using a drop-weight impact testing machine DPFest 400 (Labortech s.r.o., CZ) in accordance with the ČSN 490115 (1979) and ČSN 490117 (1980) standards, at standard temperature room (≈20 °C). The tests were conducted by releasing a 9.05 kg hammer from a height of 815.7 mm to strike the center of the specimens at a velocity of 4 m/s, inflicting 72.4 J impact energy. The position of the impacting hammer was measured with 0.01 mm accuracy. The dynamic applied force was measured by 1 MHz sampling frequency by an HBM force sensor CFTplus series with a sensing range of 30 kN to 60 kN (Hottinger Brüel & Kjaer, Austria) located on the hammer. The schematic of the impact test is shown in Fig. 1.

The machine recorded the dynamic applied force vs. time and also force vs. displacement. The charts of the dynamic applied force were cut using a filter for the duration before contact of the hammer and the specimens. The time and displacement before contacting the hammer was shifted and the start of the contact was considered zero value. The absorbed energy was automatically measured by the testing machine, calculated as the integral of the area under the force versus displacement curve for each specimen. Subsequently, the IBS could be calculated using the specimens' dimensions. The IBS was calculated using Eq. 1 to account for the dimensions of the specimens (Moreira et al. 2017).

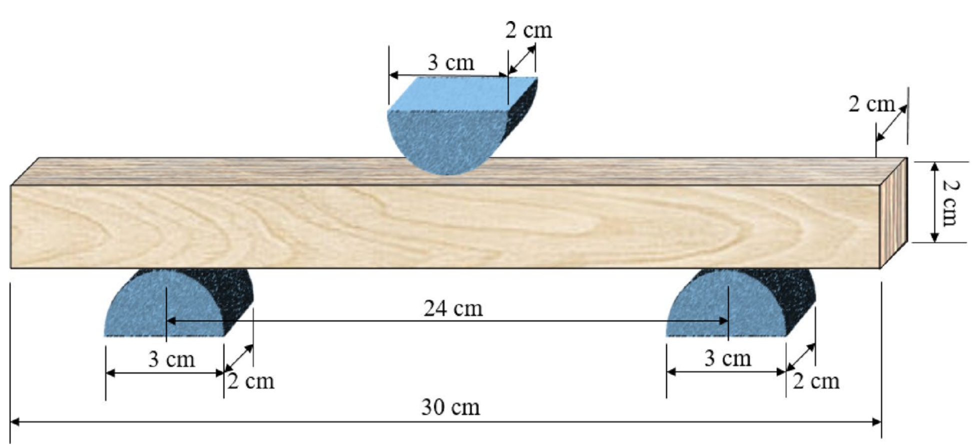

Fig. 1 Impact test setting

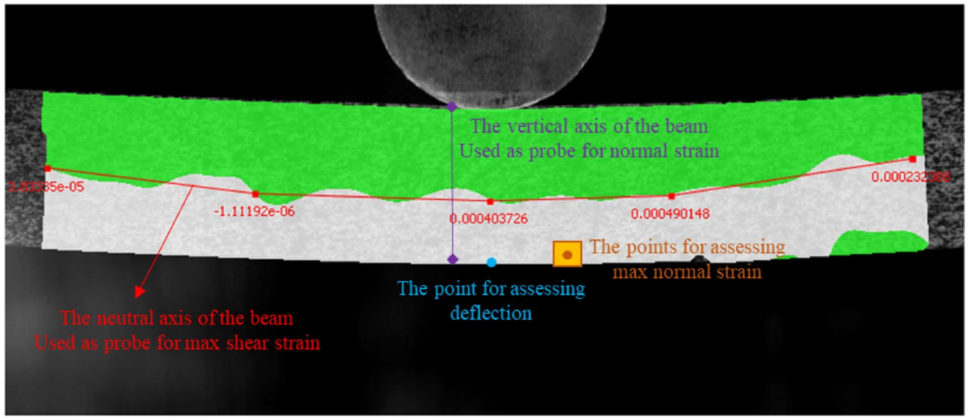

Fig. 2 Location of the probes for assessing the strain distribution

Table 1 Physical properties of the specimens and their test results

Species	Number of samples	Weight (g)	Dried weight (g)	Density (kg/m3)	MC (%)	MAX deflection (mm)	Max Strain	Max force (*N*)	IBS (J/cm^2)
Birch	14	82.9 (1.8%)	74.5 (1.7%)	676.7 (1.8%)	11.4 (1.0%)	8.9 (24.7%)	0.013 (22.3%)	6676 (20.0%)	6.8 (27.9%)
Black locust	31	81.0 (6.8%)	72.1 (7.6%)	670.6 (6.9%)	11.3 (3.5%)	7.1 (23.9%)	0.013 (24.6%)	10492 (38.5%)	7.1 (46.4%)

$$\text{IBS} = \frac{absorbed\ energy\ (J)}{height\ \times\ width\ of\ the\ sample\ (m^2)} \tag{1}$$

2.3 DIC equipment utilization

The impacts were recorded at 50,000 frames per second with a resolution of 768 × 328 pixels using a high-speed camera positioned perpendicular to the surface of the beam. The camera was FASTCAM SA-X2 type 1000 K-M2 (Photron Cameras, Japan) fitted with a Micro-Nikkor G lens (Nikon, Japan). A set of two high-speed MultiLED QT lights provided the necessary uniform light for the recording.

The recorded images were subsequently processed using DIC software Vic-2D v. 2010 (Correlated Solutions Inc., USA). The strain tensor was computed using Lagrange notation. A 1D scale calibration method was used to determine the conversion factor. The software produced the final results in the form of normal and shear strain distribution, maximum strain and deflection up to crack initiation, and strain vs. time and deflection vs. time for the tests.

The deflection was measured by selecting the midpoint of the samples, which was considered the maximum deflection point. However, assessing the maximum normal strain by selecting a single point proved problematic due to high noise levels. By choosing a small area around the points of the point which crack initiates, the maximum normal strain can be determined (Hassan Vand et al. 2024). The DIC software was used also to determine the normal longitudinal strain from the top to the bottom of the beam, as well as the shear strain along the neutral axis (Hassan Vand and Tippner 2023). The method for calculating strain and determining the probe locations is illustrated in Fig. 2. In the figure, the green region indicates compressive normal strain, while the white region is under tensile strain. The red line approximates the neutral axis, and the purple vertical probe assesses the normal strain across the specimen's thickness. Due to a high concentration of compressive strain near the hammer impact point but not at the symmetric line of the specimens, the probe locations were slightly offset from the actual symmetric line of the beam.

3 Results and discussion

The test results can be summarized by measuring the physical properties of the specimens and analysing the test outputs. Table 1 displays the physical properties and test results, with medians reported alongside standard deviations, where standard deviations are presented as a percentage of the median.

Figure 3 depicts both wood species' deflection and tensile normal strain throughout the impact duration. These charts highlight the similarities in the patterns between the two species.

Figure 4 depicts the specimens' maximum deflection and maximum normal tensile strain up to crack initiation, obtained using the DIC. Regarding strain, only tensile strain was considered in the analysis since crack initiation consistently initiated from points in the bottom of the beams which are under tension, despite compressive strain in the wood typically begins earlier due to compressive stress (Hassan Vand et al. 2024).

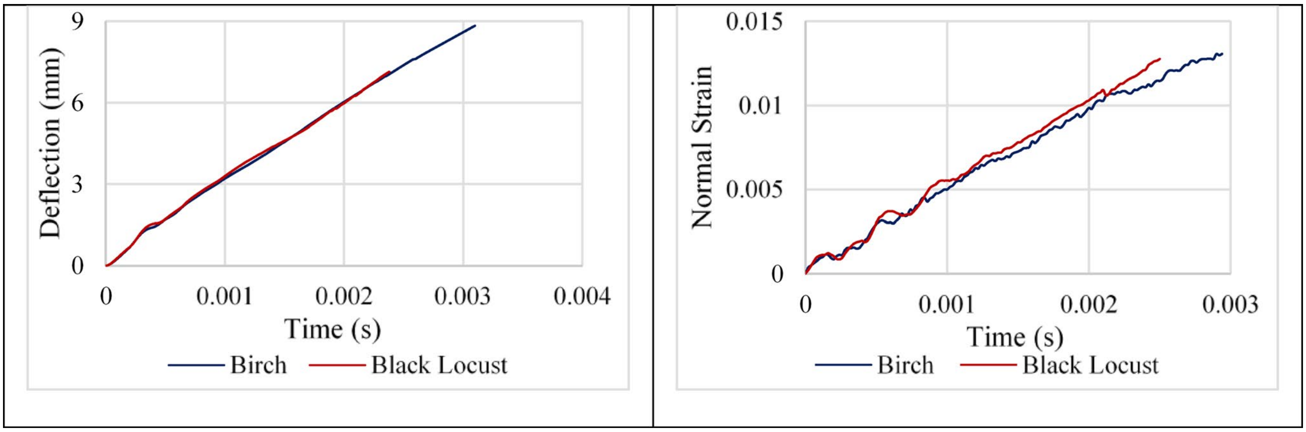

Fig. 3 Median of the deflection vs. time and normal strain vs. time of both species

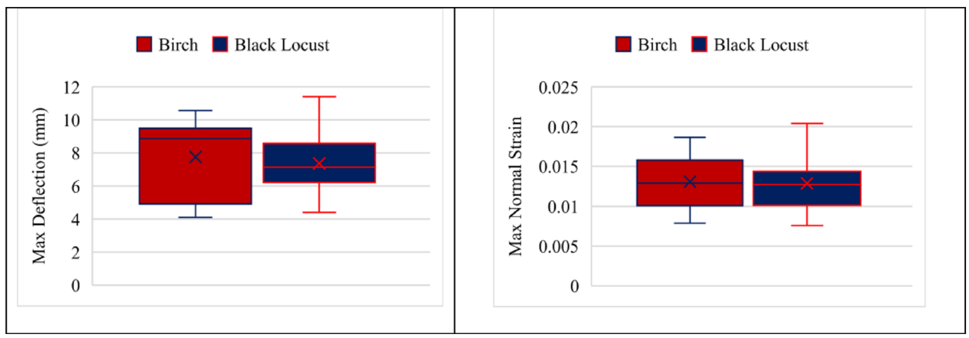

Fig. 4 Max deflection and normal strain of both species up to crack initiation

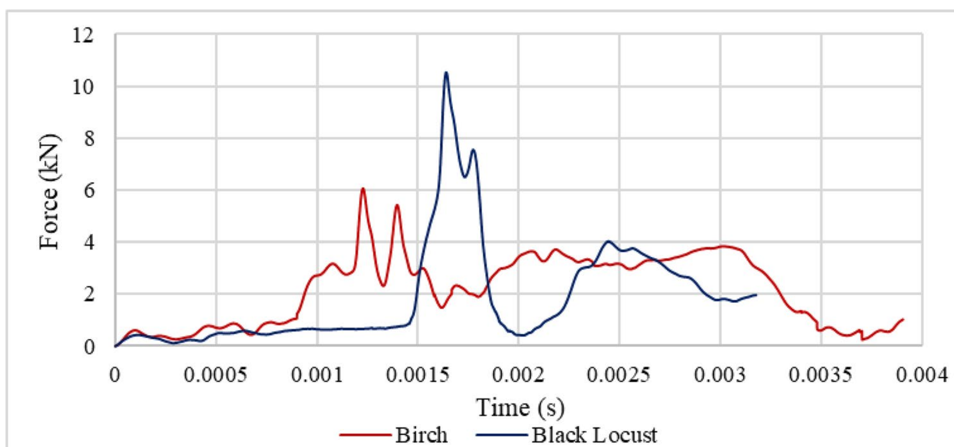

Fig. 5 Force vs. time for both species

The dynamic applied force was measured throughout the impact duration, and the force vs. time charts for both species are depicted in Fig. 5. It is important to note that the radial and tangential orientations of the growth rings do not influence the force patterns (Hassan Vand and Tippner 2024). The charts of the tests have a considerable variation, making the median of them not close to any of them, and the median of the charts just offers a general behaviour of the specimens as an approximate pattern.

The maximum dynamic applied force of the specimens and the IBS results from the tests are presented in Fig. 6. Both species show similar IBS charts, with comparable medians and variations. However, the difference in maximum force is more pronounced.

The similarity in the boxplot charts of maximum normal strain, maximum deflection, IBS, and maximum force between the two species prompted us to investigate further. A Shapiro-Wilk test, performed using MATLAB (MathWorks, USA), indicated that the data from the various result groups were not normally distributed. Therefore, we conducted statistical analysis using the Kruskal-Wallis test (MATLAB (MathWorks, USA)) instead of the classic

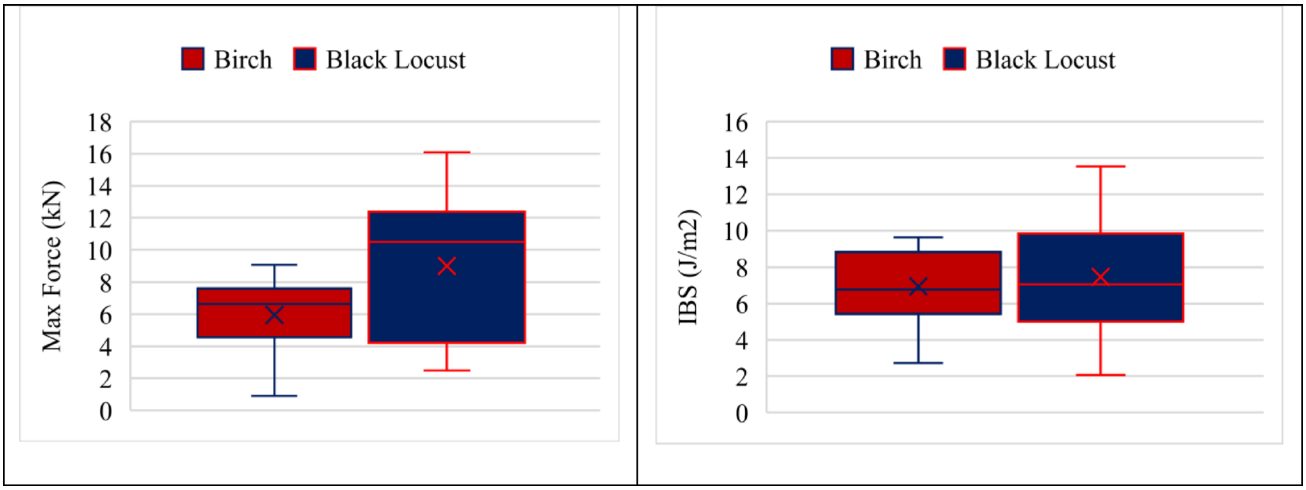

Fig. 6 Max inflicted force and the IBS of the species

Table 2 Comparative aspect of the IBS of this study and former studies

		Density (kg/m3)	difference (%)	IBS (J/cm^2)	difference (%)
Nasir and Mahmood (2007)	Black locust	737	10	8.6	21.2
Sikora et al. (2022)	Black locust	790	17.9	10.8	51.3
Kamperidou et al. (2016)	Black locust	781	16.4	-	-
Brischke (2017)	Black locust	770 (0% MC)	27	8.1	13.5
Baumann et al. (2020)	Birch	586	13.3	18.0	165
Borůvka et al. (2019)	Birch	652	3.5	8.1	19.6
Borůvka et al. (2018)	Birch	650	3.8	7.9	16.7

ANOVA test. Using the Kruskal-Wallis test, we found that the p-value for all test results except the maximum force was higher than 0.05. This indicates that the two species behave significantly similarly under impacts, demonstrating similar efficiency.

To the best of the authors' knowledge, DIC has not been previously used to assess the impact testing of birch and locust under similar conditions. Consequently, there is no suitable basis for comparing the obtained DIC results with those of previous studies. However, while DIC parameters have not been previously compared, IBS has been measured in some earlier studies. Given that IBS is not affected by dimension, it is possible to compare these results with previous research. All the modes of failure of the specimens in this study were the flexure one (with no shear mode of failure). Table 2 presents the results from former studies on the impact testing of both species and highlights the differences as calculated relative errors. Density variations were relatively low, at 10–27% for black locust and 3.5–13% for birch. However, IBS showed a wider difference: 14–51% for black locust and 17–165% for birch. Most IBS values were within the expected variability (up to 21%), but two sources (Sikora et al. 2022; Baumann et al. 2020) presented values very distant from the current study's findings.

Figures 7 and 8 depict both species' normal and shear strains under different impact levels, defined by out of plane deflections of 2, 4, and 6 mm. These figures have great potential for validating the modelling of birch and black locust using analytical and finite element methods. The normal strain distribution appears symmetric relative to the central vertical line of the specimen. The strain is highest at the bottom of the central region and decreases as one moves toward the higher regions, reaching zero at the neutral axis of the sample. Beyond the neutral axis, the strain transitions into the compressive strain region, peaking near the impact area with an absolute value significantly greater than the tensile strain. This pattern is consistent with former studies' results (Hassan Vand and Tippner 2024). For shear strain, the absolute values of the strain distribution show a symmetric pattern relative to the central vertical line but with opposite signs. The shear strain shows two small regions of differing negative values near each other beneath the hammer.

The average of results of the normal strains across the thickness (vertical profile) and the shear strains along the neutral axis (Fig. 2) for both species are shown in Fig. 9. In these charts of Fig. 9, the longitudinal axis represents the length of the probe based on the percentage, indicating the variation of strains along the length of the probes. As depicted in Fig. 9, birch demonstrates superior deformability under compression, whereas both species exhibit similar deformability in tension. Furthermore, birch registers higher shear strains than black locust. Notably, both species

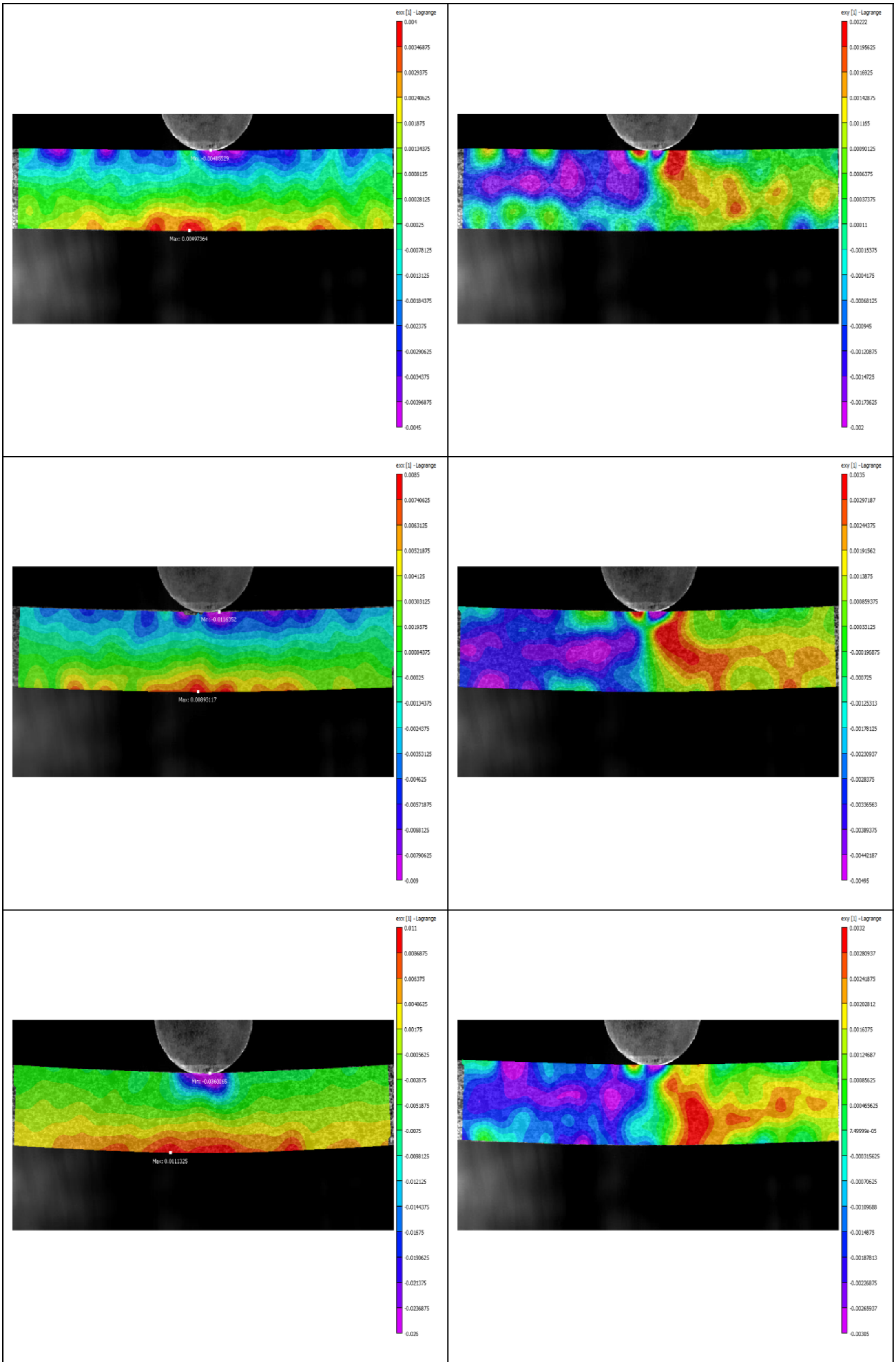

Fig. 7 Strain distribution of birch for deflections of 2, 4, and 6 mm (from top to bottom)

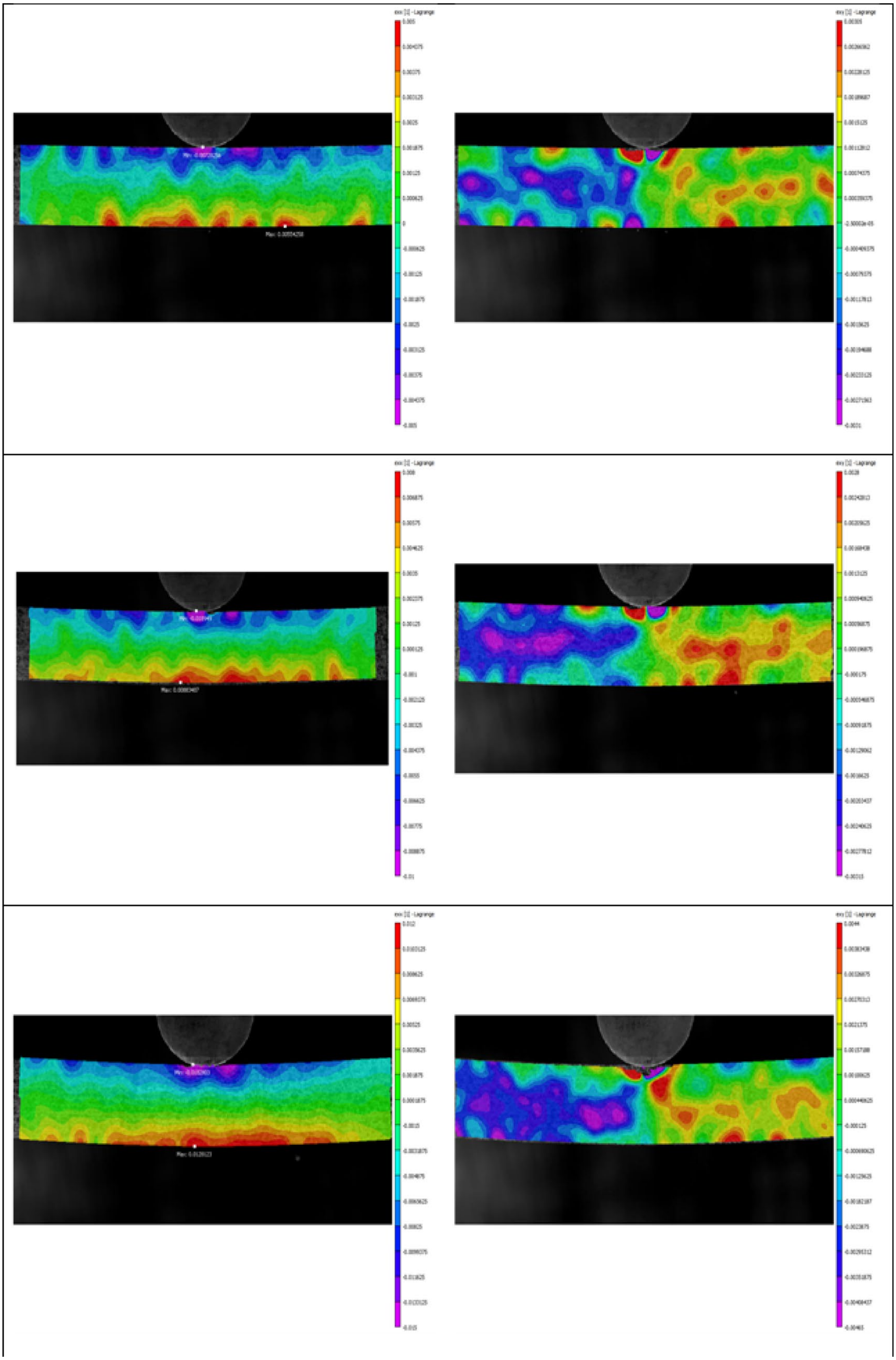

Fig. 8 Strain distribution of black locust for deflections of 2, 4, and 6 mm (from top to bottom)

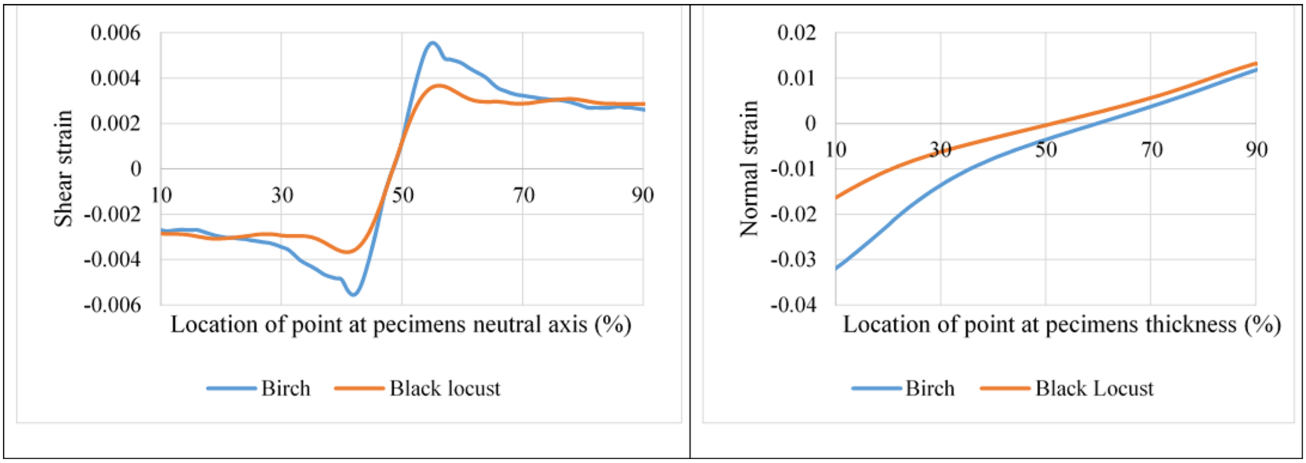

Fig. 9 Shear strain profile on the neutral axis and the normal strain profile on the vertical axis for birch and black locust at the level of crack initiation

displayed elevated normal strain during compression when contrasted with their performance in tension.

4 Conclusion

This article investigated the mechanical properties of two wood species, black locust and birch, under dynamic loading conditions. The DIC technique proved to be highly informative regarding the impact behaviour of both species, providing comprehensive insights into specimen deformation during different deflection levels. The results revealed that the maximum deflection for birch and black locust was 8.9 mm and 7.1 mm, respectively, while both species exhibited the same value of 0.013 for normal tensile strain. The IBS of brich and black locust was 6.8 and 7.0 J/cm^2, respectively. Surprisingly, the analysis of variance showed that the maximum deflection, max normal strain and IBS of both birch and black locust have negligible differences, showing they behave similarly under impacts despite their structural differences. The strain distribution offered by this article showed a clear pattern for the behavior of these species. Ultimately, this study demonstrates the potential of integrating DIC with experimental testing via impact tester device as a valuable approach for investigating complex behaviors of wood under impact loading.

Acknowledgements This work was supported by the Ministry of Education Youth and Sports in the Czech Republic (Grant Number #LL1909, ERC CZ).

Author contributions Both authors wrote the main manuscript and reviewed the manuscript.

Funding Open access publishing supported by the institutions participating in the CzechELib Transformative Agreement.

Data availability No datasets were generated or analysed during the current study.

Declarations

Competing interests The authors declare no competing interests.

References

Adamopoulos S (2002) Flexural properties of black locust (Robinia Pseudoacacia L.) small clear wood specimens in relation to the direction of load application. Eur J Wood Prod 60(5):325–327

Adamopoulos S, Passialis C, Voulgaridis E (2007) Strength properties of juvenile and mature wood in black locust (Robinia Pseudoacacia L). Wood Fiber Sci 241–249

Bal BC (2021) Effect of span length on the impact bending strength of Poplar and pine woods. Bioresour 16(2):4021

Bak M, Nemeth R (2012) Modification of wood by oil heat treatment. In International Scientific Conference March (Vol. 26, p. 27)

Baumann G, Brandner R, Müller U, Kumpenza C, Stadlmann A, Feist F (2020) Temperature-related properties of solid Birch wood under quasi-static and dynamic bending. Materials 13(23):5518

Baumann G, Brandner R, Müller U, Stadlmann A, Feist F (2021) A comparative study on the temperature effect of solid birch wood and solid beech wood under impact loading. Materials 14:7616

Beck P, Caudullo G, de Rigo D, Tinner W (2016) Betula pubescens and other birches in Europe: distribution, habitat, usage and threats. Eur Atlas For Tree Species 2985:70

Bijak S, Lachowicz H (2021) Impact of tree age and size on selected properties of black locust (*Robinia pseudoacacia* L.) wood. Forests 12(5):634

Biziks V, Andersons B, Beļkova Ļ, Kapača E, Militz H (2013) Changes in the microstructure of birch wood after hydrothermal treatment. Wood Sci Technol 47:717–735

Borůvka V, Zeidler A, Holeček T, Dudík R (2018) Elastic and strength properties of heat-treated beech and birch wood. Forests 9(4):197

Borůvka V, Dudík R, Zeidler A, Holeček T (2019) Influence of site conditions and quality of birch wood on its properties and utilization after heat treatment. Part I—elastic and strength properties, relationship to water and dimensional stability. Forests 10(2):189

Bragov A, Lomunov AK (1997) Dynamic properties of some wood species. Le J De Phys IV 7(C3):C3–487

Bragov AM, Lomunov AK, Sergeichev IV, Gray III (2006), July G. T. Dynamic behaviour of birch and sequoia at high strain rates. In AIP Conference Proceedings Vol. 845. American Institute of Physics. No. 1, pp 1511–1514.

Bragov A, Gonov M, Konstantinov A, Lomunov A, Yuzhina T (2020) Deformation and destruction at deformation rate of order 10 3 s – 1 in wood of hardwood trees. Developments and Novel Approaches in Nonlinear Solid Body Mechanics, pp 443–451

Brischke C (2017) Interrelationship between static a Nd dynamic strength properties of wood and its structural integrity. Drvna Industrija 68(1):53–60

Cao AS, Houen M, Frangi A (2024) Impact loading of glued laminated timber beams without finger-joints. Comput Struct 296:107278

Csordós D, Németh R, Bak M (2014) Variation of colour properties between and within new Robinia varieties with enhanced growing rates from different sites. BioResources 9(4):7099–7108

Dave MJ, Pandya TS, Stoddard D, Street J (2018) Dynamic characterization of biocomposites under high strain rate compression loading with split Hopkinson pressure bar and digital image correlation technique. Int Wood Prod J 9(3):115–121

Dudík R, Borůvka V, Zeidler A, Holeček T, Riedl M (2020) Influence of site conditions and quality of Birch wood on its properties and utilization after heat treatment. Part II—surface properties and marketing evaluation of the effect of the treatment on final usage of such wood. Forests 11(5):556

Dünisch O, Richter HG, Koch G (2010) Wood properties of juvenile and mature heartwood in *Robinia pseudoacacia* L. Wood Sci Technol 44(2):301–313

Field JE, Walley SM, Proud WG, Goldrein HT, Siviour CR (2004) Review of experimental techniques for high rate deformation and shock studies. Int J Impact Eng 30(7):725–775

Gaff M, Ruman D, Borůvka V, Záborský V (2016) Impact bending strength as a function of selected factors. BioResources 11(4):9880–9895

Gilman EF, Watson DG (1994) Robinia Pseudoacacia black locust. Fact sheet ST-570, a series of the environmental horticulture department. Florida Cooperative Extension Service, Institute of Food and Agricultural Sciences, University of Florida

Górszczyk J, Malicki K, Zych T (2019) Application of digital image correlation (DIC) method for road material testing. Materials 12(15):2349

Grinins J, Andersons B, Irbe I, Andersone I, Meija-Feldmane A, Janberga A, Sansonetti E (2016) Thermo-hydro treated (THT) birch veneers for producing plywood with improved properties. Holzforschung 70(8):739–746

Grünewald H, Böhm C, Quinkenstein A, Grundmann P, Eberts J, von Wühlisch G (2009) Robinia Pseudoacacia L.: a lesser known tree species for biomass production. Bioenergy Res 2:123–133

Guélou R, Eyma F, Cantarel A, Rivallant S, Castanié B (2023) A comparison of three wood species (poplar, Birch and oak) for crash application. Eur J Wood Wood Prod 81(1):125–141

Hassan Vand M, Tippner J (2023a) Impact bending strength of thermally-modified timber. Holzforschung 77(11–12):828–837

Hassan Vand M, Tippner J (2023b) Assessing shear strain distribution in wood under impact using the digital image correlation method. Int J-Wood Des Technol 12(1):1–7

Hassan Vand M, Tippner J (2024) The effect of moisture content over the fibre saturation points on the impact strength of wood. Royal Soc Open Sci 11(2):231685

Hassan Vand M, Tippner J, Brabec M (2024) Effects of species and moisture content on the behaviour of solid wood under impact. Eur J Wood Product 82(1):23–34

Hepworth DG, Vincent JF, Stringer G, Jeronimidis G (2002) Variations in the morphology of wood structure can explain why hardwood species of similar density have very different resistances to impact and compressive loading. Philos Trans R Soc Lond 360(1791):255–272

Heräjärvi H (2004) Static bending properties of Finnish Birch wood. Wood Sci Technol 37(6):523–530

Jacques E, Lloyd A, Braimah A, Saatcioglu M, Doudak G, Abdelalim O (2014) Influence of high strain rates on the dynamic flexural material properties of Spruce pine Fir wood studs. Can J Civ Eng 41(1):5664

Jansson B (1992) Impact loading of timber beams (Doctoral dissertation, University of British Columbia)

Johnson W (1986) Historical and present-day references concerning impact on wood. Int J Impact Eng 4(3):161–174

Jonczak J, Jankiewicz U, Kondras M, Kruczkowska B, Oktaba L, Oktaba J, Sut-Lohmann M (2020) The influence of Birch trees (Betula spp.) on soil environment–A review. For Ecol Manag 477:118486

Kamperidou V, Barboutis I, Vassiliou V (2016) Prospectsfor the Utilization of Black locust Wood (Robinia pseudoacacia L.) coming fromplantations in Furniture Manufacturing. In: Proceedings of the 27thInternational Conference on Wood Modification and Technology. 13th–14thOctober. Zagreb, Croatia, pp 123–128

Keunecke D, Novosseletz K, Lanvermann C, Mannes D, Niemz P (2012) Combination of X-ray and digital image correlation for the analysis of moisture-induced strain in wood: opportunities and challenges. Eur J Wood Prod 70(4):407–413

Matsushita AK, Gonzalez D, Wang M, Doan J, Qiao Y, McKittrick J (2020) Beyond density: mesostructural features of impact resistant wood. Mater Today Commun 22:100697

Moilanen CS, Saarenrinne P, Engberg BA, Björkqvist T (2015) Image-based stress and strain measurement of wood in the split-Hopkinson pressure bar. Meas Sci Technol 26(8):085206

Moreira AP, Silveira ED, Almeida DHD, Almeida THD, Panzera TH, Christoforo AL, Rocco FA (2017) Toughness and impact strength in dynamic bending of wood as a function of the modulus of elasticity and the strength in compression to the grain. Int J Mater Eng 7(4):61–67

Nasir GM, Mahmood I (2007) Properties and utilization potential of locally grown Robinia (Robinia pseudo-Acacia) wood. Pakistan J For 57:2

Nicolescu VN, Hernea C, Bakti B, Keserű Z, Antal B, Rédei K (2018) Black locust (Robinia Pseudoacacia L.) as a multi-purpose tree species in Hungary and Romania: a review. J For Res 29:1449–1463

Niklas KJ (1997) Mechanical properties of black locust (Robinia pseudoacacia) wood: correlations among elastic and rupture moduli, proportional limit, and tissue density and specific gravity. Ann Bot 79(5):479–485

Pan B, Qian K, Xie H, Asundi A (2009) Two-dimensional digital image correlation for in-plane displacement and strain measurement: a review. Meas Sci Technol 20(6):062001

Pierron F, Sutton MA, Tiwari V (2011) Ultra high speed DIC and virtual fields method analysis of a three point bending impact test on an aluminium bar. Exp Mech 51:537–563

Polocoșer T, Kasal B, Stöckel F (2017) State-of-the-art: intermediate and high strain rate testing of solid wood. Wood Sci Technol 51:1479–1534

Rédei KM, Osváth-Bujtás Z, Veperdi I (2008) Black locust (Robinia Pseudoacacia L.) improvement in hungary: a review. ACTA SILVATICA ET LIGNARIA HUNGARICA: an international journal in forest. Wood Environ Sci 4(1):127–132

Sikora A, Hájková K, Jurczyková T (2022) Degradation of chemical components of thermally modified Robinia Pseudoacacia L. wood and its effect on the change in mechanical properties. Int J Mol Sci 23(24):15652

Sitzia T, Cierjacks A, de Rigo D, Caudullo G (2016) Robinia Pseudoacacia in europe: distribution, habitat, usage and threats. European atlas of forest tree species, 166–167

Sutton MA, Orteu JJ, Schreier H (2009) Image correlation for shape, motion and deformation measurements: basic concepts, theory and applications. Springer Science & Business Media, Berlin

Thuvander F, Sjödahl M, Berglund LA (2000) Measurements of crack tip strain field in wood at the scale of growth rings. J Mater Sci 35:6267–6275

Vítková M, Müllerová J, Sádlo J, Pergl J, Pyšek P (2017) Black locust (Robinia pseudoacacia) beloved and despised: A story of an invasive tree in central Europe. For Ecol Manag 384:287–302

Wight N, Viau C, Heffernan P (2024) Behaviour of glued-laminated timber beams under impact loading. Can J Civ Eng 51(7):753–768

Wight N, Viau C, Heffernan P (2025) Cold temperature effects on the impact behaviour of glued-laminated timber beams. Int J Impact Eng 195:105–135

Wouts J, Haugou G, Oudjene M, Coutellier D, Morvan H (2016) Strain rate effects on the compressive response of wood and energy absorption capabilities–Part A: experimental investigations. Compos Struct 149:315–328

Yin H, Sedighi Moghaddam M, Tuominen M, Dėdinaitė A, Wålinder M, Swerin A (2021) Non-fluorine surface modification of acetylated birch for improved water repellence. Holzforschung 75(9):857–868

Younis FAAA, Govina JK, Seidu H, Németh R (2023) Basic characteristics of black locust (Robinia Pseudoacacia L.) wood grown under different site conditions: A review = különböző Termőhelyeken Nőtt Akác (Robinia Pseudoacacia L.) Faanyagának Alapvető jellemzői: áttekintés. ACTA SILVATICA ET LIGNARIA HUNGARICA: AN INTERNATIONAL JOURNAL IN FOREST. WOOD Environ Sci 19(1):21–35

Zink AG, Davidson RW, Hanna RB (1995) Strain measurement in wood using a digital image correlation technique. Wood Fiber Sci, 346–359

Publisher's note Springer Nature remains neutral with regard to jurisdictional claims in published maps and institutional affiliations.